

Article

The Influence of Time Domain on Flood Season Segmentation by the Fisher Optimal Partition Method

Yanbin Li, Yubo Li, Kai Feng , Ke Sun and Zhichao Cheng

College of Water Conservancy, North China University of Water Resources and Electric Power, Zhengzhou 450045, China; liyb101@163.com (Y.L.); lybacademic@163.com (Y.L.); 18110226302@163.com (K.S.); 18134006418@163.com (Z.C.)

* Correspondence: fengk0121@163.com

Abstract: Setting the staged flood limit water level (FLWL) through flood season staging is an important means of fully utilizing reservoir flood resources. The widely-used Fisher optimal partition method requires a certain time domain as the basic unit in determining the optimal staging of a flood season. Currently, 5 and 10 days matching the month and solar terms are usually used as the time unit. This study aimed to analyze the influence of other time-domain units (7 and 15 days) that meet the relevant requirements on the staging results and to provide a scientific basis for the selection of time-domain units in flood season staging. The rationality of the staging scheme was tested using the improved Cunderlik method, and the influence of specific basic units in the Fisher optimal partition method on the staging results was evaluated. The highest relative superiority of 0.9876 was found for 5 d, indicating that this is a suitable time-domain unit. The optimal staging result was determined as 20 June for the first segmentation point and 20 August for the second. A comparison of the staged FLWL with a single fixed FLWL showed that the water level was raised by 1.56 m in the pre-flood season, 0.65 m in the main flood season, and 1.37 m in the post-flood season. Water storage increased by 12.79 million m³ during the flood season, effectively alleviating the mismatch between water supply and storage.

Keywords: flood season segmentation; Fisher optimal partition; rationality examination; time-domain; flood limited water level



Citation: Li, Y.; Li, Y.; Feng, K.; Sun, K.; Cheng, Z. The Influence of Time Domain on Flood Season Segmentation by the Fisher Optimal Partition Method. *Water* **2024**, *16*, 580. <https://doi.org/10.3390/w16040580>

Academic Editor: Sajjad Ahmad

Received: 23 December 2023

Revised: 7 February 2024

Accepted: 12 February 2024

Published: 16 February 2024



Copyright: © 2024 by the authors. Licensee MDPI, Basel, Switzerland. This article is an open access article distributed under the terms and conditions of the Creative Commons Attribution (CC BY) license (<https://creativecommons.org/licenses/by/4.0/>).

1. Introduction

As an important natural resource, water is necessary for human survival and provides important support for economic and social progress [1]. As society has developed, the demand for water resources in various industries has increased, and the discrepancy between the supply and demand of water resources is becoming increasingly acute [2]. Owing to the uneven distribution of rainfall in time and space, it can be difficult to meet the water demand at certain times of the year and to balance the water demand of separate regions. As an important artificial water storage source, reservoirs can effectively improve the uneven temporal and spatial distribution of water resources [3,4]. In China, reservoirs are designed to meet the safety requirements of preventing large floods by storing water resources only up to a fixed flood limit water level (FLWL) during the flood season [5–7]. According to the Chinese Flood Control Act, the FLWL of reservoirs should not be kept high during the flood season to provide sufficient capacity for the floods that may be encountered, and is the most significant parameter in the trade-off between flood safety and water supply efficiency [8]. However, in the operation of most reservoirs, the storage capacity reserved for lowering the water level to FLWL intended to withstand more significant floods is often effective only for small and medium floods, making it difficult to address the increasingly prominent problem of conflicting water supply and demand [9]. Therefore, to improve the reservoir's water storage capacity and fully considering the various characteristics of

rainfall and flooding during the flood season, the flood season was divided into several stages to set specific segmented FLWLs without increasing flood control risks.

Flood season staging is of great significance to the operation and application of reservoirs to better understand the characteristics of incoming water and seasonal features, more accurately grasp the risk of flooding, and under the premise of safeguarding all kinds of safety, further enhance the ability to utilize flood resources, improve the ability to cope with drought disasters, and also lay the foundation for a more healthy and sustainable development of power generation, shipping, and ecology. Liu, et al. (2015) [10] delineated the seasonal FLWL through an analysis of flood season staging outcomes, maximizing benefits in flood control, power generation, and navigation. Ma, et al. (2020) [11] optimized the early FLWL with full consideration of the characteristics of flood season staging, realized the balance of the comprehensive benefits of flood control and power generation and fish spawning, and provided technical support for ecological environmental protection. In Li, et al. (2022) [12], based on the staging results considering risk and benefit indicators, the FLWL selection scheme integrating water supply and power generation and extreme risk is identified, which lays a scientific foundation for further improving the benefits of water supply and power generation.

Methods for flood season segmentation have undergone gradual development from the qualitative method of causative analysis [13,14] and further quantitative methods of statistical and fuzzy analysis based on historical storm floods, to the new methods of more refined and rigorous quantification [15]. The main staging methods can be summarized as follows: (1) The clustering method classifies various categories by finding the smallest difference within a class. Mo, et al. (2018) [16] considered the effect of climate change, used the Set Pair Analysis Method (SPAM) for flood season segmentation, and determined the staged FLWL. Ju, et al. (2020) [17] used an improved fuzzy set analysis method based on the normal distribution theory to stage the flood season of cascade reservoirs downstream of Jinshajiang River. (2) The change-point method uses the flood hydrological elements as a time series, based on statistical theory, to find a series of sudden changes and as a division of the time series of excessive and staging points. Liu, et al. (2010) [18] used two types of segmentation models that depended on either the annual maximum (AM) or the peaks-over-threshold (POT) method of sampling, applied the probability change-point analysis technique for flood staging, and used Monte Carlo experiments to evaluate the performance of these models. (3) The ensemble-method approach is coupled with various staging methods and combines the advantages of each method to make the flood stage staging results more reasonable. Jiang, et al. (2019) [19] used an integrated dynamic fuzzy C-mean clustering validity function and genetic algorithm, which objectively determined the optimal number of clusters to achieve flood staging. Jiang, et al. (2015) [20] used an ensemble-method approach of fuzzy clustering methods, probability change point analysis, and statistical graph techniques to provide a more reasonable segmentation than the individual methods.

The Fisher optimal partition method is a statistical method for the cluster analysis of ordered samples, which considers multiple factors and maintains the original sample order. It is widely used in flood season staging [19,21,22]. Most current studies improve the Fisher optimal partition method by assigning different index weights, such as expert scoring method assignment [23], fuzzy hierarchical analysis method assignment [24], entropy weighting method assignment [25], and so on. Yu, et al. (2021) [26] compared commonly used indicator-weighting algorithms and concluded that the weights have only a minor influence on the staging results. Therefore, investigating the indicator weights for the Fisher optimal partition method is not of significant importance. However, the method as applied in flood staging uses a certain time domain as the basic unit for cluster optimization. This will make the application of the method somewhat subjective in time domain selection. At present, when the Fisher optimal partition method is applied to the staging of flood season in China, the time-domain units are generally chosen to be 5-day [27] and 10-day [28]. The reason for choosing 5-day and 10-day units is that as the traditional

Chinese timekeeping units, they are better matched with the months and more in line with the seasonal characteristics of agricultural activities. For the selection of the time domains, Xu and Niu (2019) [29] used the Fisher optimal partition method with 5-day and 10-day time units in the flood staging of the Zhangjiazhuang Reservoir and found that the delay of the main flood season increased by 15 days when using the 5-day time unit. This was thought to be the reason that the gap within the sample class was smaller and more refined when the 5-day time unit was used. This assessment, which is directly based on gaps in staging results, is subjective and requires further quantitative analysis and research. Therefore, whether it is reasonable to take 5 or 10 days as the basic unit of the Fisher optimal partition method, and what the specific impact is of the selection of a wider time domain on the staging results are of great significance and research value for the application and promotion of the Fisher optimal partition method in flood season staging. The innovation inherent in this study lies in its investigation of the temporal domain's influence on the Fisher optimal partition method within the context of flood season staging. This endeavor contributes a scientific foundation to facilitate a more discerning and rational application of the method, thereby advancing its scientific and practical utility.

In order to further investigate the effect of different time domains on the Fisher's most segmented method in flood season staging, we chose a time interval of 7 days, between 5 days and 10 days, as the basic time unit. In addition, a time domain of 15 days was chosen to extend the time domain scope of the study. The above time domains are well matched with the months, which is in line with the characteristics of flood management and seasonality. Therefore, in this study, the time domains of 5, 7, 10, and 15 d were used as time units, and four flood staging schemes were obtained from the Fisher optimal partition method through an example investigation of flood staging for the JianGang Reservoir. The rationality of the staging results in specific time domains was evaluated using the rationality test method [30], and the influence of the staging results was analyzed. The optimal staging scheme was determined, the staged FLWL was extrapolated, and the water supply benefits of the staged FLWL were evaluated and compared with those of a single fixed FLWL. These research ideas and methods provide a reference base for research into and application for similar problems.

2. Materials and Methods

2.1. Study Area and Data

The JianGang Reservoir is located upstream of the Jialu River in the Shaying River system of the Huai River Basin (Figure 1). The dam is located west of JianGang Village in Zhengzhou City, with a controlled drainage area of 113 km² and a total reservoir capacity of 60,704,100 m³. The area is near the Yellow River Basin, which is at the edge of China's warm temperate semi-humid monsoon climate region. It has four distinct seasons controlled by Pacific subtropical high pressure in summer and autumn, with common southeast winds and hot, rainy conditions. It is controlled by Siberian and Mongolian high pressure systems in winter and spring, with prevailing northwest winds, a dry climate, and little rain. Precipitation is unevenly distributed within the year and between years, with an average annual rainfall of approximately 640 mm. Approximately 90% of the annual rainfall is concentrated in the flood season of June, July, August, and September, with storms occurring mostly in July and August.

The basic data used in this study are the daily rainfall data from 1970 to 2017 for the JianGang Reservoir and the measured flood data after the establishment of the JianGang Reservoir in 1970. Relevant data and information were obtained from the JianGang Reservoir Management Office. A statistical analysis of daily rainfall data was performed for the selection of indicators for the staging of the flood season. The reservoir was designed and constructed to meet the design flood standard of a one-in-100-year event and the calibration flood standard of a one-in-5000-year event. The design flood level was set at 153.01 m, and the calibration flood level was set at 156.47 m. Rainfall in the JianGang Reservoir study area is mainly concentrated between June and September, and the flood

season is from 1 June to 30 September according to the JianGang Reservoir Management Office operational programme.

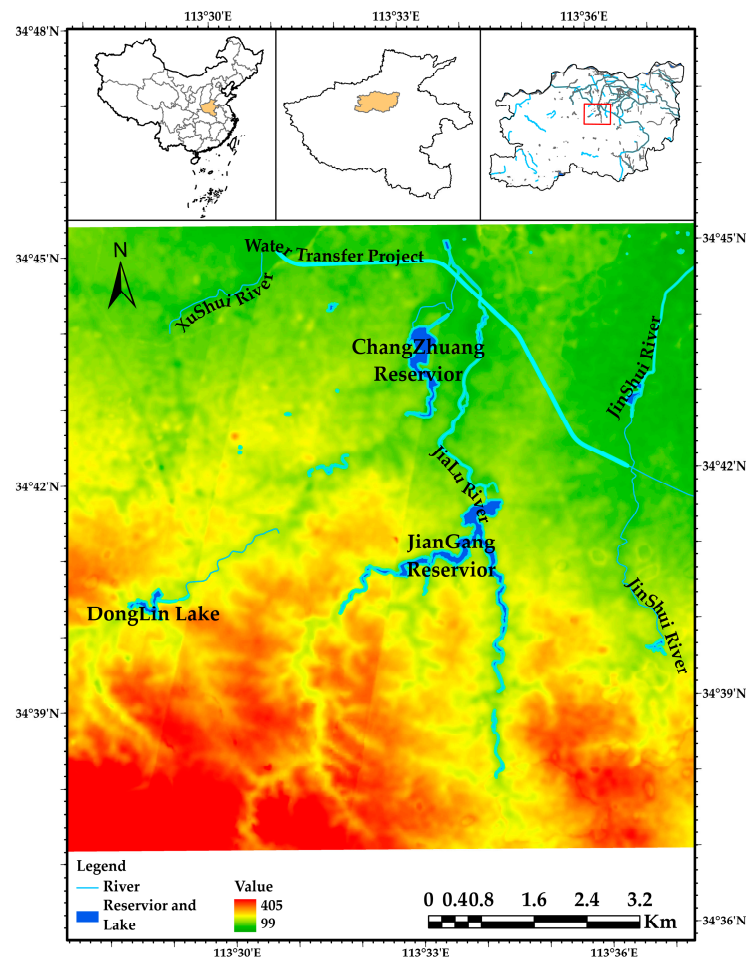


Figure 1. Map of the study area. Note: The colored image corresponds to the enlarged view within the red box.

2.2. Fisher Optimal Partition Method

2.2.1. Concept

The Fisher optimal partition method is used to cluster a sequence of ordered time samples, and is based on the minimum square sum of the sample total deviation, with the smallest difference within the class and the maximum difference between the classes [22]. As a cluster analysis method for ordered samples, it allows for the consideration of several factor indicators and the determination of the optimal number of segments and flood season segmentation results according to the defined objective function, without destroying the original order.

2.2.2. Steps of Calculation

Processing the data. Based on n samples arranged in a certain order, each with m factor indicators, an ordered sample, and a relationship matrix x_{ij} (where $i = 1, 2, \dots, n$, and $j = 1, 2, \dots, m$) constructed using multi-factor indicators, X . The physical quantities of each indicator are of different magnitudes and cannot be compared directly. Therefore, it is necessary to transform the characteristic values of the indicators so that they are dimensionless, then obtain the standardized characteristic matrix x'_{ij} .

$$x'_{ij} = \frac{x_{ij} - x_{\min,j}}{x_{\max,j} - x_{\min,j}} \quad (1)$$

where x'_{ij} is the characteristic value of the index after normalization, and $x_{max,j}$ and $x_{min,j}$ are the maximum and minimum values of x_{ij} in the j th index, respectively.

Determining the objective weight by entropy weight. The entropy weighting method determines the degree of disorder and information effectiveness of the information by calculating the information entropy based on the information of influencing factors. The positive correlation between the entropy value and the effective information provided by the index value also indicates the level of the weight value [24]. It is calculated using the following equations [25]. Based on the determined relationship matrix X , it was normalized to calculate the index information entropy S_j .

$$S_j = -\frac{1}{\ln n} \sum_{i=1}^n \frac{x'_{ij}}{x_j} \ln \left(\frac{x'_{ij}}{x_j} \right) \quad (2)$$

$$x_j = \sum_{i=1}^n x'_{ij} \quad (3)$$

where $i = 1, 2, \dots, n, j = 1, 2, \dots, m$, S_j is the information entropy of the j th influencing factor, and x_j is the sum of the n information values of the j th factor. The weights of the influencing factors were calculated.

$$\omega_j = \frac{1 - s_j}{m - \sum_{j=1}^m s_j} \left(0 \leq \omega_j \leq 1, \sum_{j=1}^m \omega_j = 1 \right) \quad (4)$$

Each indicator is assigned specific weight coefficients $\omega_1, \omega_2, \dots, \omega_m$ according to its importance to the sample classification, and the matrix of multi-indicator eigenvalues can be transformed into a one-dimensional eigenvalue vector Y after the weighted average, as follows:

$$Y = \begin{pmatrix} y_1 \\ \vdots \\ y_n \end{pmatrix} = \begin{pmatrix} x'_{11} & \cdots & x'_{1m} \\ \vdots & \ddots & \vdots \\ x'_{n1} & \cdots & x'_{nm} \end{pmatrix} \begin{pmatrix} \omega_1 \\ \vdots \\ \omega_m \end{pmatrix} \quad (5)$$

where Y is used as the initial vector after the weighting assignment for which the sample sequence is segmented.

Defining the class diameter. The degree of difference among classes is expressed by the class diameter. The smaller the difference among the samples, the smaller is the class diameter. Suppose the class $p = y_i, y_{i+1}, \dots, y_j$ ($j > i$); then, the average value of class p can be found as follows:

$$\bar{y}_p = \frac{1}{j - i + 1} \sum_{\alpha=i}^j y_\alpha \quad (6)$$

Assuming that $D(i, j)$ denotes the class diameter of class p , $D(i, j)$ can be determined from the mean \bar{y}_p of class p .

$$D(i, j) = \sum_{\alpha=i}^j (y_\alpha - \bar{y}_p)^2 \quad (7)$$

Defining the objective function. If n ordered time samples are divided into k classes, $B'(n, k)$ is defined as one of the classification methods, and its computational formula is expressed as follows:

$$B'(n, k) = \sum_{\alpha=1}^k D(i_\alpha, i_{\alpha+1} - 1) \quad (8)$$

where the minimum value of $B'(n, k)$ is the optimal classification method. Therefore, the objective function $B(n, k)$ is defined as follows:

$$B(n, k) = \min B'(n, k) = \min \sum_{\alpha=1}^k D(i_{\alpha}, i_{\alpha+1} - 1) \quad (9)$$

The calculation of $B(n, k)$ has the following recursive process.

$$k = 2, B(n, 2) = \min_{2 \leq i \leq n} \{D(1, i - 1) + D(i, n)\} \quad (10)$$

$$k > 2, B(n, k) = \min_{k \leq i \leq n} \{D(i - 1, k - 1) + D(i, n)\} \quad (11)$$

Determining the optimal segmentation. When objective function $B(n, k)$ is found, the ordered sample can be divided into k classes. To determine the optimal number of segments, a graph of the objective function $B(n, k)$ and the number of segments k is constructed, where the inflection is the optimal number of segments. The degree of change in the slope $\gamma(k)$ of the graphed curve is determined. We calculated $\gamma(k)$ using the following formula:

$$\gamma(k) = |B(n, k) - B(n, k - 1)| \quad (12)$$

Then, the graph of $\gamma(k)$ and the number of segments k is plotted, where the maximum position is that of maximum change; that is, the optimal number of segments.

2.3. Reasonability Analysis

Chen, et al. (2015) [30] improved the Cunderlik, et al. (2004) [31] method of dividing abundance and depletion by month for the whole year, and introduced a fuzzy superiority function to quantitatively evaluate the rationality of flood staging. A more quantitative and accurate evaluation of staging results [18,27,32,33] is widely used compared to the results of multiple staging methods. Li, et al. (2021) [34] used the modified Cunderlik method for reasonability analysis based on rainfall data when classifying flood and non-flood periods. Therefore, this study analyzed the reasonability of the staging results of basic units in various time domains based on daily rainfall data at the JianGang Reservoir from 1970 to 2017. The basic calculation steps are as follows, see Chen, et al. (2015) [30] for specific formula details:

- (1) For the rainfall leading to floods during the flood season, it is assumed that the probability of rainfall occurring on any day of the flood season is equal and random, and obeys a uniform distribution. The number of rainfalls occurring in each phasing stage is counted by stochastic simulation and then its relative frequency is calculated.
- (2) Determine the upper and lower frequencies of the uniformly distributed confidence interval based on the magnitude of the relative frequencies.
- (3) Relative frequency values for each staging scenario for the Point Reservoir were determined using a nonparametric bootstrap sampling method.
- (4) Determine the relative affiliation of the phases in all scenarios based on their generalized distances.
- (5) The fuzzy relative superiority value is calculated based on the relative affiliation to further compare the reasonableness of the staging scheme.

2.4. Calculation of the Staged FLWL

The design flood process method was used for each phase in accordance with the maximum value of the intertemporal sampling method. The cumulative empirical frequency of each phase of the flood peak series was calculated using the P-III type frequency curve. Then, the design flood of each phase was determined. According to the typical flood process, various initial and diversion water levels were formulated, and the flood

regulation calculation was performed according to the reservoir capacity and discharge relationship of the reservoir water level using the following formula:

$$\frac{Q_1 + Q_2}{2} \Delta t - \frac{q_1 + q_2}{2} \Delta t = V_1 - V_2 \quad (13)$$

where $q = f_1(Z)$; $V = f_2(Z)$; Q_1 and Q_2 indicate the reservoir inflow at the beginning and end of the period (m^3/s); q_1 and q_2 are the discharge flows at the beginning and end of the period (m^3/s), respectively; V_1 and V_2 are the water storage capacities of the reservoir at the beginning and end of the period (m^3); Δt is the calculation period (s); and Z is the water level (m).

Based on the results of the flood diversion calculation, the FLWL of each stage was determined by selecting the highest initial water level that met the flood control requirements in each stage.

2.5. Methodology Flow Chart

To elucidate the methodological logic, we presented a technical roadmap in Figure 2, aiming to provide a visual representation of the research methodology's sequential flow.

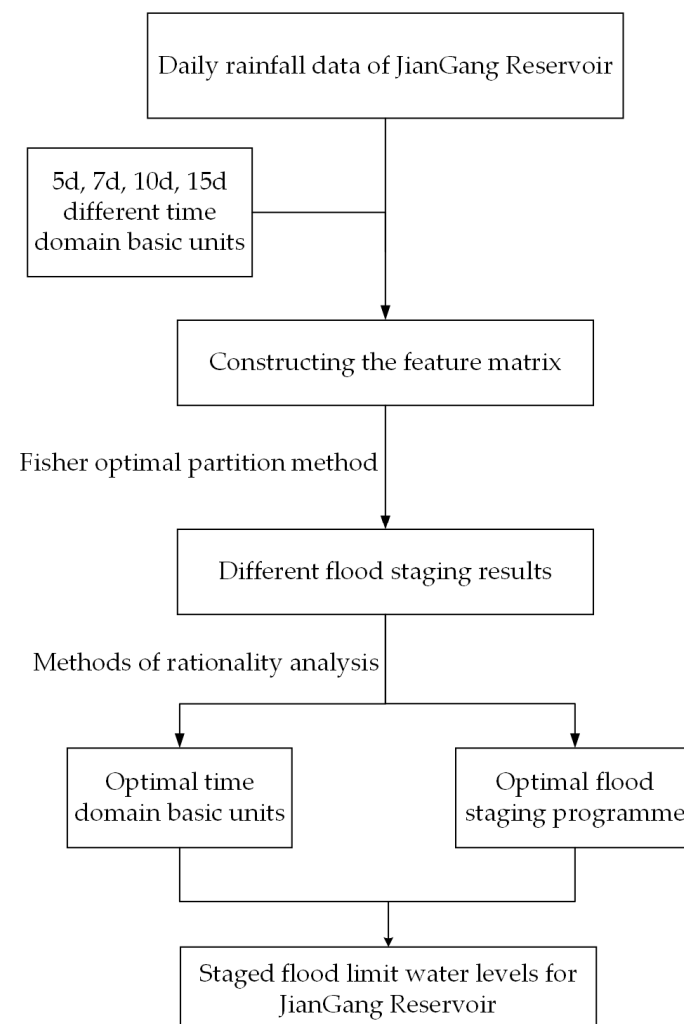


Figure 2. Method flow chart of the staged flood limit level for JianGang Reservoir considering time domain effects.

3. Results

3.1. Flood Season Segmentation

3.1.1. Entropy Weighting Method to Calculate Weights

Based on the independence and seasonal screening of rainfall indicators, Li, et al. (2021) [34] used the gray correlation method to consider the independence, informativeness, and seasonal characteristics of the indicators, and selected multiple indicators for analysis, and the study concluded that the multi-year average total rainfall, the multi-year average maximum 3-day rainfall, and the average multi-year maximum 1-day rainfall have strong correlation, so a more representative indicator is selected for analysis. The basic data used for the calculation of the feature matrix are the daily rainfall data of the JianGang Reservoir from 1970 to 2017. Relevant data and information were obtained from the JianGang Reservoir Management Office. In this study, the multi-year average maximum 1-day rainfall (determined by the maximum value of the annual average rainfall in this section, referred to in the text as Q_1), maximum number of rainfall days (determined by the number of times the annual rainfall maximum occurs in this section, referred to in the text as Q_2), and the multi-year average rainfall CV value (CV denotes the coefficient of variation of rainfall, determined by the ratio of the multi-year rainfall distance median to the multi-year average rainfall, and referred to in the text as CV) of the three indicators are selected to construct the characteristic matrix for the flood season staging. The feature matrix with 5 d as the base unit for example is shown in Table 1.

Table 1. The feature matrix with 5 d as the base unit.

N	Q_1	Q_2	CV
1	22.1	0	1.65
2	47.3	0	1.27
3	64	2	1.70
4	30.1	0	1.73
5	164.8	2	1.52
6	67.1	2	1.55
7	117.8	3	1.47
8	109.7	4	1.36
9	167.6	1	1.44
10	125.5	3	1.41
11	143.5	5	1.56
12	112.5	3	1.18
13	145	1	1.38
14	79.1	3	1.59
15	101.4	5	1.28
16	73.5	4	1.53
17	92.5	1	1.35
18	77.6	2	1.61
19	65.4	0	1.41
20	107.6	1	1.69
21	76.4	4	2.47
22	82.6	2	1.82
23	55.9	0	2.04
24	38.5	0	1.74

Taking 5 d as the basic unit of the time domain as an example, the feature matrix was normalized using Equation (1) and based on the feature matrix data. Then, the weights of the three indicators were calculated by the entropy weighting method using Equations (2)–(4). The resulting weight values of Q_1 , Q_2 , and CV were $\omega_{5d} = (0.3238, 0.2124, 0.4638)$. Using the entropy weighting method to find the weight of the three indicators range from 0.2124 to 0.4638, the indicator weights do not differ much, indicating that the indicator is more able to respond to the seasonal characteristics of the flood season. This aligns with the findings that the weights allocated to the five indicators through Xia, et al. (2019) [25]'s

employment of the entropy weighting method exhibit minimal variations. The rationale behind the application of the entropy weighting method in assessing the objectivity of information entropy weighting is thereby substantiated as reasonable. This suggests that the chosen index information is not only representative but also highly responsive to the seasonal characteristics of the JianGang Reservoir area. The selection of indicators with prominent seasonal characteristics and fewer correlations to construct a representative matrix has an important impact on the rationality and representativeness of the staging results. Consequently, a robust and representative feature matrix has been constructed, laying a solid foundation for the subsequent staging of the flood season.

3.1.2. Fisher Optimal Partition

The requested weight value ω was substituted into formula (5) to obtain Y . Then, according to Equations (6) and (7), the class diameter $D(i, j)$ was obtained according to $D(i, j)$ through Formulas (10) and (11) to calculate the objective function $B(n, k)$, and through Equation (12) to find the optimal segmentation node. The results are shown in Table 2 and the full table is available in the Supplementary Materials.

Table 2. Calculation results of the objective function $B(n, k)$.

k	n									
	2	3	4	5	6	7	8	9	...	23
3	0.0001 (3)	-	-	-	-	-	-	-	...	-
4	0.0103 (3)	0.0001 (4)	-	-	-	-	-	-	-	-
5	0.0321 (5)	0.0103 (5)	0.0001 (5)	-	-	-	-	-	-	-
6	0.0412 (5)	0.0194 (5)	0.0092 (5)	0.0001 (6)	-	-	-	-	-	-
7	0.0538 (5)	0.0319 (5)	0.0194 (7)	0.0092 (7)	0.0001 (7)	-	-	-	-	-
8	0.0684 (5)	0.0418 (7)	0.0199 (7)	0.0098 (7)	0.0007 (7)	0.0001 (8)	-	-	-	-
9	0.0765 (5)	0.0546 (5)	0.0344 (7)	0.0199 (9)	0.0098 (9)	0.0007 (9)	0.0001 (9)	-	-	-
10	0.0787 (5)	0.0568 (5)	0.0367 (7)	0.0222 (9)	0.0120 (9)	0.0029 (9)	0.0007 (10)	0.0001 (10)	-	-
11	0.1844 (5)	0.0787 (11)	0.0568 (11)	0.0367 (11)	0.0222 (11)	0.0120 (11)	0.0029 (11)	0.0007 (11)	-	-
12	0.1886 (5)	0.1110 (11)	0.0787 (12)	0.0568 (12)	0.0367 (12)	0.0222 (12)	0.0120 (12)	0.0029 (12)	-	-
13	0.2016 (5)	0.1526 (11)	0.0804 (12)	0.0585 (12)	0.0384 (12)	0.0239 (12)	0.0138 (12)	0.0047 (12)	-	-
14	0.2052 (5)	0.1692 (11)	0.0811 (12)	0.0592 (12)	0.0391 (12)	0.0247 (12)	0.0145 (12)	0.0054 (12)	-	-
15	0.2203 (5)	0.1793 (11)	0.0992 (12)	0.0773 (12)	0.0572 (12)	0.0391 (15)	0.0247 (15)	0.0145 (15)	-	-
16	0.2222 (5)	0.1844 (7)	0.1006 (12)	0.0787 (12)	0.0586 (12)	0.0437 (15)	0.0292 (15)	0.0191 (15)	-	-
17	0.2776 (5)	0.2222 (17)	0.1401 (12)	0.1006 (17)	0.0787 (17)	0.0586 (17)	0.0437 (17)	0.0292 (17)	-	-
18	0.2806 (5)	0.2312 (17)	0.1419 (12)	0.1096 (17)	0.0877 (17)	0.0676 (17)	0.0527 (17)	0.0382 (17)	-	-
19	0.4014 (5)	0.2589 (17)	0.2211 (17)	0.1373 (17)	0.1096 (19)	0.0877 (19)	0.0676 (19)	0.0527 (19)	-	-
20	0.4248 (5)	0.2640 (17)	0.2263 (17)	0.1425 (17)	0.1185 (19)	0.0966 (19)	0.0765 (19)	0.0615 (19)	-	-
21	0.5681 (5)	0.4248 (21)	0.2640 (21)	0.2263 (21)	0.1425 (21)	0.1185 (21)	0.0966 (21)	0.0765 (21)	-	-
22	0.5767 (5)	0.4785 (21)	0.3178 (21)	0.2640 (22)	0.1962 (21)	0.1425 (22)	0.1185 (22)	0.0966 (22)	-	-
23	0.6432 (5)	0.5207 (17)	0.4134 (21)	0.2728 (22)	0.2350 (22)	0.1512 (22)	0.1272 (22)	0.1053 (22)	-	-
24	0.7212 (5)	0.5578 (17)	0.4438 (22)	0.2831 (22)	0.2453 (22)	0.1615 (22)	0.1375 (22)	0.1156 (22)	...	0.0001 (24)

Note: the number in parentheses after the value of $B(n, k)$ was the splitting point i_k between the k th class and the $k-1$ th class for the current classification case.

The graphs of the objective function $B(n, k)$ versus the number of segments k , and $\gamma(k)$ versus the number of segments k are shown in Figure 3a.

Figure 3a shows that $B(n, k)$ gradually decreases with an increase in the number of segments k . There is a clear inflection at $k = 3$, which corresponds to the maximum of $\gamma(k)$. The optimal number of segments (3) was determined accordingly. Table 2 shows that the segmentation results were 1 June to 20 June for the pre-flood period, 21 June to 20 August for the main flood period, and 21 August to September 30 for the post-flood period.

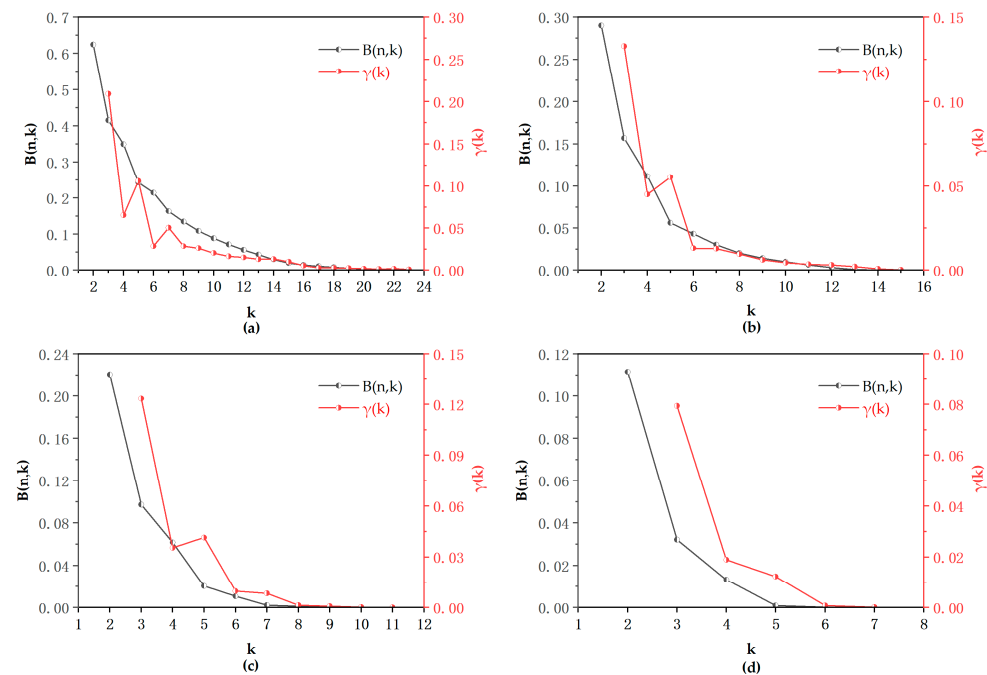


Figure 3. Relationship between $B(n,k)$, $\gamma(k)$, and k in (a) 5 d time domain, (b) 7 d time domain, (c) 10 d time domain, and (d) 15 d time domain.

As with using 5 d as the basic unit of the time domain, the same feature matrix was constructed by selecting the same feature indicators with 7, 10, and 15 d as the basic units of the time domain. The corresponding weight values were obtained by the entropy weighting method as $\omega_{7d} = (0.3888, 0.3571, 0.2541)$, $\omega_{10d} = (0.3227, 0.3792, 0.2981)$, and $\omega_{15d} = (0.2757, 0.3674, 0.3568)$. The weights were substituted into Equation (5), and the corresponding intraclass diameter $D(i,j)$ and objective function $B(n,k)$ were derived in turn. The graphs of the objective function $B(n,k)$ versus the number of segments k and $\gamma(k)$ versus the number of segments k were plotted in Figure 3b–d.

The number of segments k corresponding to the maximum value of $\gamma(k)$ according to Equation (12) is the optimal number of segments. As Figure 3b–d show, from Equation (12), with different time domain values as the basic unit, $\gamma(k)$ is maximized at $k = 3$, so the optimal numbers of segments are all 3. According to the results, it can be seen that different time domains as basic units do not affect the number of optimal staging segments. It shows that the change of time domain does not affect the trend of $B(n,k)$ and the number of segments k corresponding to the maximum value of $\gamma(k)$.

The flood staging results of the four different time domains were obtained according to the objective function $B(n,k)$ results in Table 2, as shown in Table 3.

Table 3. Summaries of the staging results by time domain.

Time Domains	Pre-Flood Season	Main Flood Season	Post-Flood Season
5 d	1 June–20 June	21 June–20 August	21 August–30 September
7 d	1 June–21 June	22 June–14 August	15 August–30 September
10 d	1 June–20 June	21 June–20 August	21 August–30 September
15 d	1 June–15 June	16 June–15 August	16 August–30 September

Based on the staging results in Table 3, it can be observed that the staging results for 5 and 10 days are the same. The staging results for the 7 d pre-flood period are relatively close to each other, but the post-flood period is advanced by 5 days compared to the 5- and 10-day periods. The main and post-flood periods for the 15 d period are both advanced by 5 days compared to the 5 d and 10 d periods. Further analysis reveals that the staging

results for 5 d and 10 d are the same, while the staging results for 7 d and 15 d differ by 6 days in the pre-flood period but only by one day in the post-flood period, which suggests a high degree of similarity between time domains where a multiplicative relationship exists.

Differences in the staging results may be due to the fixation of the time domain limiting the staging results for determining the best location. For example, in the split nodes of the pre-flood and main flood seasons, the 7 d time domain unit could only select 14 June, 21 June, and 28 June, which suggests that the $B(n, k)$ value calculated with 21 June as the first split point is more appropriate compared to the other two smaller staging results. For the 15 d time domain unit, only 15 June and 1 July could be selected as the first split point, and the $B(n, k)$ value calculated with 15 June indicated that the smaller staging result was more appropriate. The reason for the difference is that the span of the larger time domains is fixed, and more suitable staging nodes may appear in the range of time domains, which makes it impossible to be selected.

3.2. Reasonability Analysis

The theoretical frequency curves of the confidence intervals of the four schemes were obtained according to the steps determined by the upper and lower bounds of the evenly distributed confidence interval, as shown in Figure 4.

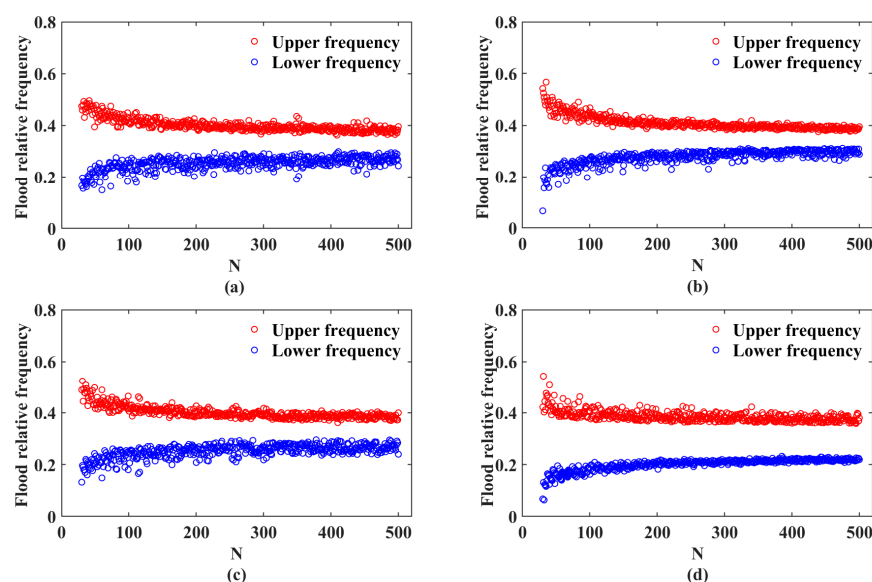


Figure 4. Graphs of relative frequency confidence for four time domains: (a) 5 d; (b) 7 d; (c) 10 d; and (d) 15 d.

Because the data used in this study are rainfall data from 1970 to 2017, the results of fitting were obtained by fitting $N = 48$ years for 5 d $y_{up} = 0.4575$, $y_{lower} = 0.1959$; 7 d $y_{up} = 0.4667$, $y_{lower} = 0.2222$; 10 d $y_{up} = 0.4621$, $y_{lower} = 0.1906$, and 15 d $y_{up} = 0.4310$, $y_{lower} = 0.1544$. According to the frequency values of the upper and lower limits, the relative membership of each stage was calculated, and the relative superiority of specific time-domain schemes was obtained according to the relative favourability formula [30], as shown in Figure 5.

According to the relative genus preference relationship of the four schemes, the genus degree of the 5-day basic unit staging was 0.9876, followed by the 10-day basic unit staging at 0.9677. The fuzzy relative superiority of both schemes exceeded 0.9, indicating an acceptable staging scheme. Therefore, it is best to use 5 d as the basic unit staging scheme for the Fisher optimal partition method. However, the fuzzy relative superiority of the 10 d scheme was comparable to the 5 d scheme, so it can also be applied to flood staging.

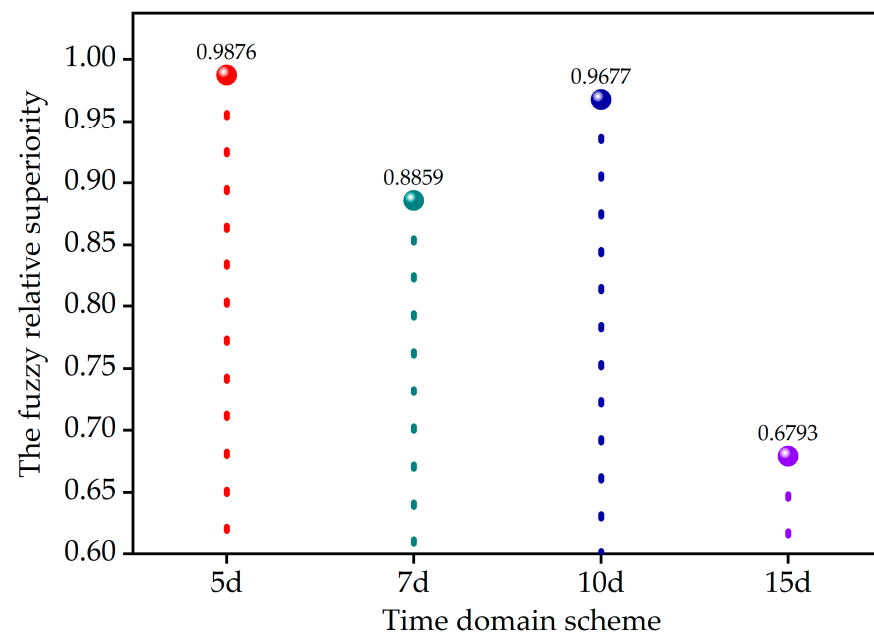


Figure 5. The fuzzy relative superiority of various time-domain schemes.

According to Table 3, there are three first-stage nodes of the pre-flood and main flood seasons: June 15, 20, and 21. There are also three second-stage nodes of the main and post-flood periods: 14, 15 and 20 August. The fuzzy relative superiority of 24 schemes fixed with three first-staging points and a series of second-staging point combinations with a gradient from 14 August to 21 August were calculated as shown in Figure 6a. The fuzzy relative superiority of the three second-staging point combinations and a series of first-staging point combinations with a series of 14 June to 21 June gradients was fixed. The results are shown in Figure 6b.

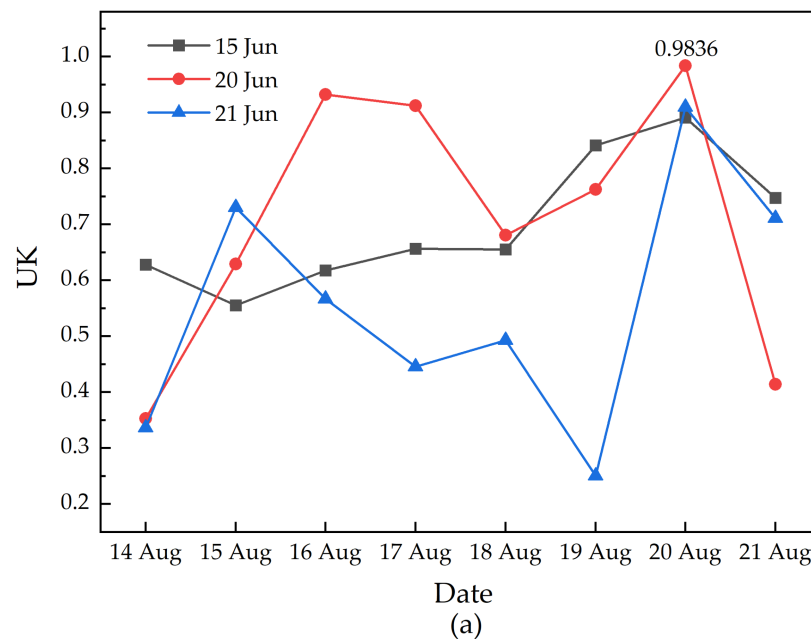


Figure 6. Cont.

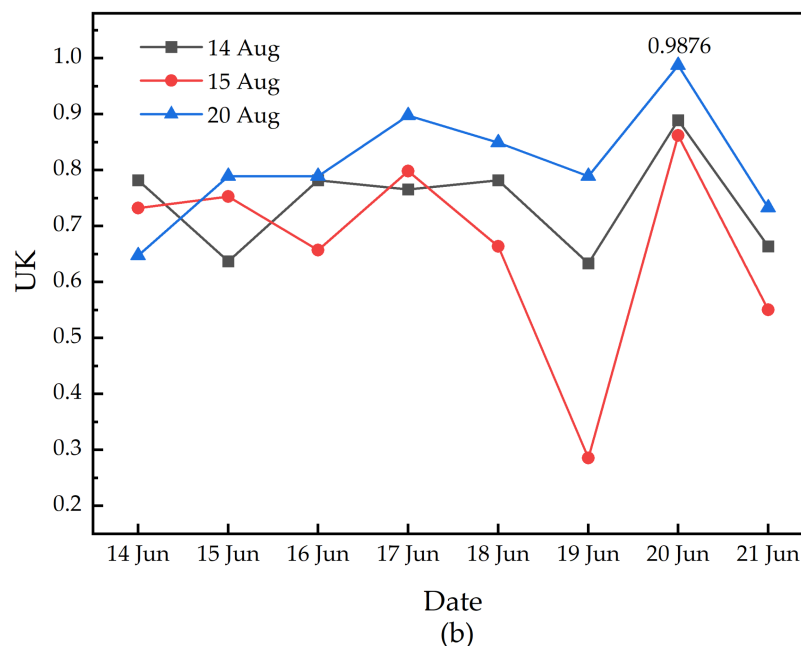


Figure 6. The fuzzy relative superiority of different staging schemes with fixed first segmentation points (a) and fixed first segmentation points (b). Note: UK is the fuzzy relative superiority of each staging result obtained through the reasonableness analysis.

Figure 6a,b show that among the three schemes with fixed first segmentation points, all have 20 August as the better second segmentation point. The scheme is optimal when the first staging node is 20 June, with a relative superiority of 0.9836. Among the three schemes with fixed second segmentation points, all have 20 June as the better first segmentation point, and the scheme is optimal when the second segmentation point is 20 August, with a relative superiority of 0.9876. In summary, the staging scheme was determined to be optimal with 20 June as the first segmentation point and 20 August as the second segmentation point. The same staging results of the Fisher optimal partition method were obtained with 5 d and 10 d as the basic units. The results demonstrate that the Fisher optimal partition method can be used for flood staging with 5 d and 10 d as the basic units, and that the staging scheme is optimal with 5 d as the basic unit. However, this was only marginally superior to the 10 d unit. Using the staging scheme with other time domains as the basic unit is not recommended.

3.3. FLWL Determination and Benefit Analysis

Table 4 shows design peak flow information for the reservoir. The hydrological series consists of a sample sequence of 1970–2017 flood data, compiled according to the annual maximum method, to form a sample capacity of 48 peak flows for each phase. Considering the maximum of the phase for appropriate intertemporal sampling, we used the mathematical expectation formula to calculate the cumulative empirical frequency of each phase of the peak flow series. We used the current hydrological frequency calculation method and the appropriate line method to derive the corresponding peak flow of the stage of the 100-year (1%) design standard and 5000-year + 15% safety guarantee value (0.008%) calibration standard.

Based on the principle of selecting the typical flood with high flood peak values, high flood volumes, and unfavourable flood defences [35], the flood process of 6 August 1975 was selected from the measured flood data as a typical flood process for projecting 100-year design standards and 5000-year +15% safety guarantee rate check standard flood processes. The design flood process was derived by scaling up the corresponding typical floods using the same ratio scaling method.

Table 4. Staged flood frequency calculation results.

	Frequency (%)	Pre-Flood Season	Main Flood Season	Post-Flood Season
Peak flow (m ³ /s)	1	566.24	903.13	636.78
	0.008	1964	2723	2018
Expectation (m ³ /s)		153.87	329.61	215.13
CV		0.7	0.5	0.55
CS/CV		3.5	3.5	3.5

Note: CV is the coefficient of variation, CS is the skewness coefficient.

Under the premise of ensuring flood control safety, the design flood level of 153.01 m and the check flood level of 156.96 m for the JianGang Reservoir were used as the control values of reservoir flood control scheduling. Various initial water levels were formulated according to a typical flood process, and the flood regulation calculation was performed according to the relationship between the reservoir water level and the discharge relationship (Figure 7) to calculate the maximum water level that did not exceed the flood control standard (Table 5).

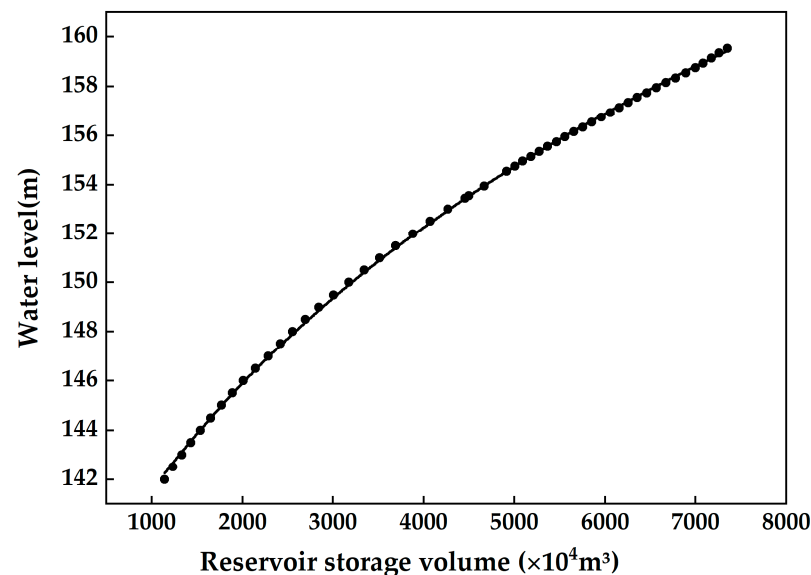


Figure 7. JianGang Reservoir stage-storage curves. Note: The black dots represent the corresponding positions of water level and storage capacity, and the curve is the fitted curve of the relationship between water level and storage capacity of the reservoir.

According to the findings presented in Table 5, when the pre-flood season initial water level is at 152.11 m and the post-flood season initial water level is recorded at 151.92 m, the computed maximum water level for the 100-year design flood precisely aligns with 153.01 m. However, the maximum water level derived from the flood regulation calculation for the 5000-year +15% safety guarantee rate check flood falls below the check flood level of 156.96 m. When the initial water level during the main flood season is 151.20 m, the computed maximum water level for the corresponding frequency flood regulation precisely matches both the design flood level and the check flood level. Consequently, under the condition of not escalating flood prevention risks, it is recommended to set the FLWL at 152.11 m for the pre-flood season, 151.20 m for the main flood season, and 151.92 m for the post-flood season.

Table 5. Operation results of each frequency and initial water levels.

Flood Frequency	Initial Water Level (m)	100-Year	5000-Year + 15%
Pre-flood season maximum water level (m)	150.55	151.57	155.12
	150.80	151.79	155.28
	151.00	151.97	155.41
	152.00	152.81	155.08
	152.10	152.99	156.14
	152.11	153.01	156.17
Main flood season maximum water level (m)	150.55	152.45	156.62
	150.85	152.70	156.78
	151.15	152.93	156.92
	151.17	152.96	156.94
	151.19	152.99	156.95
	151.20	153.01	156.96
Post-flood season maximum water level (m)	150.55	151.75	155.24
	151.00	152.15	155.53
	151.50	152.61	155.86
	151.90	152.98	156.12
	151.91	152.99	156.13
	151.92	153.01	156.14

4. Discussion

4.1. Reasonableness of Flood Season Staging and Benefits of Staged FLWL

The current operational main flood season for the JianGang Reservoir spans from 21st June to 15th August, with the FLWL set at 150.55 m [36]. The Fisher optimal partitioning method was employed to delineate the flood season phases of the JianGang Reservoir. According to the determined flood season phases from the optimal partitioning scheme, the pre-flood season spans from 1st June to 20th June, the main flood season extends from 21st June to 20th August, and the post-flood season persists from 21st August to 30th September. Upon a comparative analysis of reservoir operation schemes, it was observed that the initiation date of the main flood season, as determined by the Fisher optimal partitioning method, consistently falls on 21st June, with a conclusion on 20th August, representing a mere extension of 5 days compared to the current operational scheme. Wang, et al. (2016) [21] conducted an analysis of the impact of climate change on the flood season in the Fen River Basin, reaching the conclusion that the flood season is prolonged. Therefore, this study suggests that the observed prolongation of the main flood season in JianGang Reservoir may be attributable to climate change. The slight extension in the results of the main flood season phasing indicates that the utilization of the Fisher optimal partitioning method for flood season delineation is rational. Extending the main flood season by 5 days is regarded as a strategy to further enhance the flood safety of the reservoir during the flood season.

By implementing flood season staging for the JianGang Reservoir, it is possible to extrapolate staged flood limit levels, improve floodwater utilization efficiency, increase the economic benefits of the reservoir, and enhance the region's resilience to drought. Tang and Zhang (2018) [22] analyzed the impact of sudden rainfall changes on reservoir staging outcomes, revealing an extension of the main flood season. Furthermore, by optimizing FLWL, they enhanced reservoir storage capacity. Mo, et al. (2022) [37] analysed the seasonal characteristics of the flood season of Longtan Reservoir, proved the necessity of its flood season staging, and further increased the effective capacity of the reservoir by deducing the staged FLWL. In this paper, the results of the staged FLWL are compared with the latest optimization study conducted by Shi, et al. (2023) [36], which considers the fuzzy preference determination of the FLWL, incorporating the two decision-making preferences of flood control and water supply. The results are illustrated in Figure 7.

Figure 8 displays the result of the staged FLWL determined by the flood regulation algorithm. Shi, et al. (2023) [36]’s research findings indicate that the FLWL based on flood control preference is 151.35 m, while the FLWL based on water supply preference is 151.55 m. These levels are respectively 0.15 m and 0.25 m higher than the main flood season FLWL of 151.20 m determined in this paper, yet they remain lower than the FLWL for the pre-flood season and post-flood season. This indicates that the staged FLWL are lower during the main flood season compared to the single FLWL. Although this reduces the available water supply during the main flood season, it allows for an increase in water supply during the pre-flood season and post-flood season, thereby preventing situations where there is insufficient water storage during the post-flood season. Furthermore, the comparatively lower FLWL during the main flood season significantly enhances flood safety during this critical period [38]. By staging the flood season of the JianGang Reservoir and setting specific FLWL for each stage, compared with the original fixed FLWL of 150.55 m, the water levels were raised by 1.56 m for the pre-flood season, 0.65 m for the main flood season, and 1.37 m for the post-flood season. Under the premise of not compromising the safety of flood control, the water storage capacities were increased by 5.63 million m³ in the pre-flood season, 2.25 million m³ in the main flood season, and 4.91 million m³ in the post-flood season. Therefore, the total increase in water storage across the whole flood season could reach a maximum of 12.79 million m³. Compared with the fixed FLWL, the staged FLWL substantially increased the water storage across the flood season.

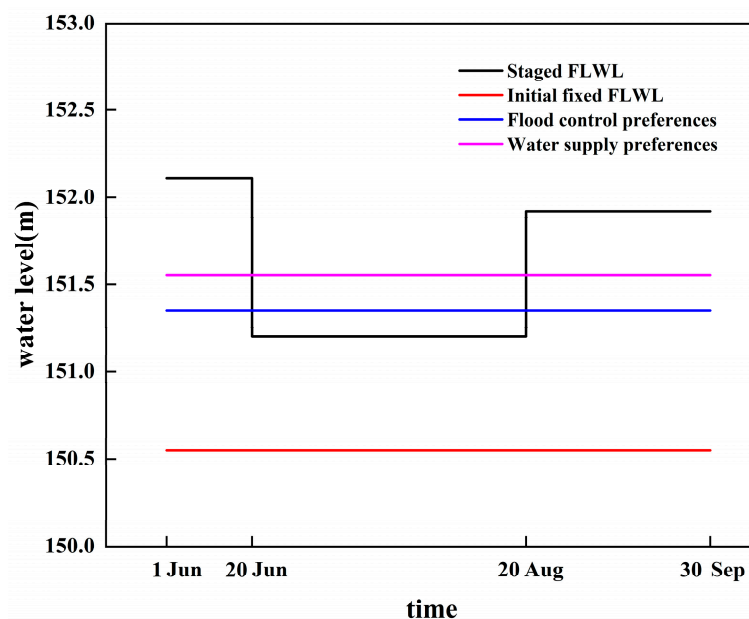


Figure 8. Optimisation and comparison results of FLWL for JianGang Reservoir. Note: Node mapping with the end date of the previous staging result.

4.2. Limitations and Applications

The selection of the time domain within the Fisher optimal partitioning method is predicated upon traditional Chinese time units of 5 d and 10 d, which align effectively with the calendrical delineation of months and festive occasions. In this study, we have opted to scrutinize the impact of time domain selection on staging outcomes by employing intervals of 7 d and 15 d, which similarly exhibit congruence with the temporal demarcation of months and solar terms. Nonetheless, it is imperative to acknowledge the current study’s limitation in not delving into an exhaustive exploration of the influence exerted by other non-standard temporal units. Furthermore, the nuanced trajectory of the temporal domain gradient and its consequential effects warrant in-depth analysis for comprehensive understanding. This study employs a rationality analysis approach to conduct a fuzzy preference analysis on the staging outcomes associated with different temporal domains.

Through the determination of preferential relationships among each staging scheme, it becomes apparent that the current selection of temporal domains may exhibit a certain degree of unilateral bias. Consequently, it is imperative to employ additional analytical frameworks for a more comprehensive examination. The findings of this analysis underscore the significance of the traditional Chinese agricultural timekeeping units of 5 d and 10 d, integral components of the traditional Chinese 24 solar terms—an ancient agrometeorological timekeeping method. Notably, the study demonstrates that these time units, with their roots in traditional Chinese agricultural practices, afford a nuanced reflection of seasonal characteristics and patterns. As such, further investigation into the seasonal patterns and inherent characteristics associated with the 5 d and 10 d units is warranted for a more nuanced understanding.

Among the commonly used staging methods, while fractal analysis theory [37] is grounded in strong physical principles, it is constrained to the consideration of a single indicator. On the other hand, the change-point analytic method [18], which can evaluate multiple objectives, is hindered by the subjectivity introduced in determining the number of variable points. The Fisher optimal partition method, as a mathematical and statistical approach capable of considering multiple indicators, is noted for its simplicity and practicality. However, its application and widespread adoption are impeded by the inherent drawback of subjectivity associated with time domain selection. Tang and Zhang (2018) [22], as well as Li and Zhou (2018) [39], have both highlighted the limitations associated with utilizing a 10 d time domain in the context of the Fisher optimal partition method. Consequently, the primary innovation of this study lies in the systematic exploration of the repercussions stemming from the selection of a time domain in the application of the Fisher optimal partition method specifically within the context of flood season staging. The analysis undertaken endeavors to meticulously examine the distinct impacts and interrelationships of varying time domains on the staging outcomes, thereby offering a scientifically grounded foundation for the judicious selection of time domains in the application of the Fisher optimal partition method for flood season staging. This endeavor seeks to address inherent subjectivity concerns associated with the method. Moreover, the findings of this research contribute not only to the optimization of time domain selection for flood season staging but also extend applicability to diverse domains. The elucidation of a scientific basis for time domain selection in the Fisher optimal partition method holds broader implications, ranging from earthquake staging [40] to meteorological statistical prediction [41], thereby enriching the method's utility in diverse scientific fields.

5. Conclusions

This study aimed to analyze the influence of various selected time-domain units on the staging results and to provide a scientific time-domain selection basis for the application of the Fisher optimal partition method in flood season staging. In this study, we selected the JianGang Reservoir as the research object and examined specific time-domain basic units used in flood season staging by the Fisher optimal partition method. We used 5, 7, 10, and 15 d time-domain basic units for flood season staging and compared them by the rationality analysis method. The research conclusions are as follows:

- (1) Through rationality analysis, the staged schemes of specific time domains were compared. It was concluded that the relative superiority of the 5-day basic unit staging reached 0.9876, followed by 0.9677 for the 10-day unit. There were only marginal differences in superiority between the 5-day and 10-day units. However, the staging scheme for the other time domains was poor. By fixing the first and second staging nodes, we compared the staged schemes to determine the best staging scheme, using 20 June as the first segmentation point and 20 August as the second segmentation point. The results show that when the Fisher optimal partition method was used for staging, the 5-day or 10-day units could be used as the basic unit for flood staging. The 5-day unit was the optimal basic unit staging scheme. Using other time domains as the basic unit for staging is not recommended.

- (2) Through the flood season stage, the staged FLWL was set for the flood season of the JianGang Reservoir, and the FLWL was determined to be 152.11 m in the pre-flood season, 151.20 m in the main flood season, and 151.92 m in the post-flood season, compared with the single FLWL of 150.55 m. The pre-flood season FLWL was raised by 1.56 m, the main flood season by 0.65 m, and the post-flood season by 1.37 m. Water storage increased by 12.79 million m³ throughout the flood season, substantially alleviating the mismatch between the supply and demand of water resources during the flood season.

Supplementary Materials: The following supporting information can be downloaded at: <https://www.mdpi.com/article/10.3390/w16040580/s1>, Table S1: Calculation results of the objective function $B(n, k)$.

Author Contributions: Y.L. (Yubo Li) and K.F. designed the study; Y.L. (Yubo Li) did the main programming and wrote the draft of the manuscript; Y.L. (Yanbin Li) and K.F. guided the research and revised the manuscript; K.S. performed data pre-processing; Z.C. assisted in data analysis and results validation. All authors have read and agreed to the published version of the manuscript.

Funding: This research was supported by the National Key Research and Development Program of China (2023YFC3006603), National Natural Science Fund of China (grant numbers 52179015 and 42301024), Science and Technology Projects in Henan Province (grant numbers 201300311400 and 222102320043), State Key Laboratory of Simulation and Regulation of Water Cycle in River Basin (grant number IWHR-SKL-KF202212), and Yinshanbeilu Grassland Eco-hydrology National Observation and Research Station, China Institute of Water Resources and Hydropower Research (grant number YSS202112).

Data Availability Statement: The data presented in this study are available on request from the corresponding author.

Conflicts of Interest: The authors declare no conflicts of interest.

References

1. Loucks, D.P.; van Beek, E. *Water Resource Systems Planning and Management*; Springer: Cham, Switzerland, 2017; p. 2017. [\[CrossRef\]](#)
2. Tan, Q.F.; Wang, X.; Liu, P.; Lei, X.H.; Cai, S.Y.; Wang, H.; Ji, Y. The Dynamic Control Bound of Flood Limited Water Level Considering Capacity Compensation Regulation and Flood Spatial Pattern Uncertainty. *Water Resour. Manag.* **2017**, *31*, 143–158. [\[CrossRef\]](#)
3. Guo, S.; Zhang, H.; Chen, H.; Peng, D.; Liu, P.; Pang, B. A reservoir flood forecasting and control system for China/Un système chinois de prévision et de contrôle de crue en barrage. *Hydrol. Sci. J.* **2009**, *49*, 959–972. [\[CrossRef\]](#)
4. Chou, F.N.F.; Wu, C.W. Expected shortage based pre-release strategy for reservoir flood control. *J. Hydrol.* **2013**, *497*, 1–14. [\[CrossRef\]](#)
5. Ding, W.; Zhang, C.; Peng, Y.; Zeng, R.; Zhou, H.; Cai, X. An analytical framework for flood water conservation considering forecast uncertainty and acceptable risk. *Water Resour. Res.* **2015**, *51*, 4702–4726. [\[CrossRef\]](#)
6. Cheng, C.; Wang, W.; Xu, D.; Chau, K.W. Optimizing Hydropower Reservoir Operation Using Hybrid Genetic Algorithm and Chaos. *Water Resour. Manag.* **2008**, *22*, 895–909. [\[CrossRef\]](#)
7. Diao, Y.; Wang, B. Scheme optimum selection for dynamic control of reservoir limited water level. *Sci. China Technol. Sci.* **2011**, *54*, 2605–2610. [\[CrossRef\]](#)
8. Li, X.A.; Guo, S.L.; Liu, P.; Chen, G.Y. Dynamic control of flood limited water level for reservoir operation by considering inflow uncertainty. *J. Hydrol.* **2010**, *391*, 126–134. [\[CrossRef\]](#)
9. Chen, J.H.; Guo, S.L.; Li, Y.; Liu, P.; Zhou, Y.L. Joint Operation and Dynamic Control of Flood Limiting Water Levels for Cascade Reservoirs. *Water Resour. Manag.* **2013**, *27*, 749–763. [\[CrossRef\]](#)
10. Liu, P.; Li, L.P.; Guo, S.L.; Xiong, L.H.; Zhang, W.; Zhang, J.W.; Xu, C.Y. Optimal design of seasonal flood limited water levels and its application for the Three Gorges Reservoir. *J. Hydrol.* **2015**, *527*, 1045–1053. [\[CrossRef\]](#)
11. Ma, C.; Xu, R.; He, W.; Xia, J. Determining the limiting water level of early flood season by combining multiobjective optimization scheduling and copula joint distribution function: A case study of three gorges reservoir. *Sci. Total Environ.* **2020**, *737*, 139789. [\[CrossRef\]](#) [\[PubMed\]](#)
12. Li, X.; Zhang, Y.; Tong, Z.; Niu, G. Reservoir Flood Season Segmentation and Risk–benefit Cooperative Decision of Staged Flood Limited Water Level. *Water Resour. Manag.* **2022**, *36*, 3463–3479. [\[CrossRef\]](#)
13. Bender, M.J.; Simonovic, S.P. A fuzzy compromise approach to water resource systems planning under uncertainty. *Fuzzy Sets Syst.* **2000**, *115*, 35–44. [\[CrossRef\]](#)

14. Singh, V.P.; Wang, S.X.; Zhang, L. Frequency analysis of nonidentically distributed hydrologic flood data. *J. Hydrol.* **2005**, *307*, 175–195. [\[CrossRef\]](#)
15. Song, Y.; Wang, H. Study on stage method of reservoir flood season. *Energy Rep.* **2022**, *8*, 138–146. [\[CrossRef\]](#)
16. Mo, C.X.; Mo, G.Y.; Liu, P.; Zhong, H.H.; Wang, D.Y.; Huang, Y.; Jin, J.L. Reservoir operation by staging due to climate variability. *Hydrol. Sci. J.* **2018**, *63*, 926–937. [\[CrossRef\]](#)
17. Ju, B.; Yu, Y.; Zhang, F.; Lei, X.; You, F. Flood season partition and flood limit water level determination for cascade reservoirs downstream jinshajiang river. *IOP Conf. Ser. Earth Environ. Sci.* **2020**, *569*, 012005. [\[CrossRef\]](#)
18. Liu, P.; Guo, S.; Xiong, L.; Chen, L. Flood season segmentation based on the probability change-point analysis technique. *Hydrol. Sci. J.* **2010**, *55*, 540–554. [\[CrossRef\]](#)
19. Jiang, H.; Wang, Z.Z.; Ye, A.L.; Liu, K.L.; Wang, X.H.; Wang, L.H. Hydrological characteristic-based methodology for dividing flood seasons: An empirical analysis from China. *Environ. Earth Sci.* **2019**, *78*, 399. [\[CrossRef\]](#)
20. Jiang, H.Y.; Yu, Z.B.; Mo, C.X. Reservoir Flood Season Segmentation and Optimal Operation of Flood-Limiting Water Levels. *J. Hydrol. Eng.* **2015**, *20*, 1–7. [\[CrossRef\]](#)
21. Wang, H.; Xiao, W.; Wang, J.; Wang, Y.; Huang, Y.; Hou, B.; Lu, C. The Impact of Climate Change on the Duration and Division of Flood Season in the Fenhe River Basin, China. *Water* **2016**, *8*, 105. [\[CrossRef\]](#)
22. Tang, L.; Zhang, Y.B. Considering Abrupt Change in Rainfall for Flood Season Division: A Case Study of the Zhangjia Zhuang Reservoir, Based on a New Model. *Water* **2018**, *10*, 1152. [\[CrossRef\]](#)
23. Liu, K.; Wang, Y.; Hu, S.; Gao, B. Application of Fisher optimal dissection method to flood season division. *Adv. Sci. Technol. Water Resour.* **2007**, *27*, 14–16+37.
24. Zhu, Y.; Wu, P. Application of FAHP-Fisher Optimal Dissection Method in Flood Season Division. *Water Resour. Power* **2016**, *34*, 57–59+56.
25. Xia, Q.; Li, Y.; Guo, J.; Wang, L.; Lin, W. Application of Improved Fisher Optimal Partition Method Based on Entropy Weight Method to Flood Season Division of Reservoir. *Pearl River* **2019**, *40*, 42–47.
26. Yu, H.; Liu, X.; Wu, X.; Wang, Y.; Wang, J.; Peng, S. The Influence of the Weight of Index Algorithm on the Fisher's Optimal Segmentation in the Reservoir's Flood Season. *China Rural. Water Hydropower* **2021**, *1*, 105–110.
27. Zhou, K. Flood season segmentation and scheme optimization in the Yellow River. *J. Water Clim. Chang.* **2022**, *13*, 274–286. [\[CrossRef\]](#)
28. Mo, C.; Wang, D.; Zhu, X.; Ruan, Y.; Mo, G.; Lin, Y. Application of Fisher Optimal Partition on Flood Season Staging in Chengbihe Reservoir. *Water Power* **2017**, *43*, 19–22+27.
29. Xu, Y.; Niu, X. Study on the Influence of Different Domains on Flood Season Division Based on Improved Optimal Dissection Method. *Water Power* **2019**, *45*, 19–22.
30. Chen, L.; Singh, V.P.; Guo, S.L.; Zhou, J.Z.; Zhang, J.H.; Liu, P. An objective method for partitioning the entire flood season into multiple sub-seasons. *J. Hydrol.* **2015**, *528*, 621–630. [\[CrossRef\]](#)
31. Cunderlik, J.M.; Ouarda, T.B.M.J.; Bobée, B. On the objective identification of flood seasons. *Water Resour. Res.* **2004**, *40*, 1–12. [\[CrossRef\]](#)
32. Chen, L.; Pan, Z.; Liu, W.; Teng, X. Flood Season Staging and Its Rationality Verification for Longtan Hydropower Station. *Water Power* **2019**, *45*, 17–21.
33. Sun, G.; Liu, S.; Wang, G.; Du, T.; Mo, C. Application of Improved Fuzzy Set Analysis Method in Flood Season Staging and Its Rationality. *Water Power* **2020**, *46*, 4–8.
34. Li, J.; Song, S.; Wang, H. Determining Flood Season Based on Index Screening and Rationality Analysis of Division Results. *J. Basic Sci. Eng.* **2021**, *29*, 123–134. [\[CrossRef\]](#)
35. Ge, H.; Huang, Z.; Wang, Y.; Li, J. Application of Fuzzy Optimization Model Based on Entropy Weight in Typical Flood Hydrograph Selection. *J. Hydrol. Eng.* **2013**, *18*, 1400–1407. [\[CrossRef\]](#)
36. Shi, J.; Duan, Z.; Wang, J.; Ge, W. Research on the Adjustment Method of Flood Limit Water Level Considering the Overall Risk of City-Reservoir. *Yelltwo River* **2023**, *45*, 70–74. [\[CrossRef\]](#)
37. Mo, C.; Deng, J.; Lei, X.; Ruan, Y.; Lai, S.; Sun, G.; Xing, Z. Flood Season Staging and Adjustment of Limited Water Level for a Multi-Purpose Reservoir. *Water* **2022**, *14*, 775. [\[CrossRef\]](#)
38. Liu, P.; Guo, S.; Xiao, Y.; Li, W.; Xiong, L. Study on the optimal reservoir seasonal flood control water level. *J. Hydroelectr. Eng.* **2007**, *26*, 5–10.
39. Li, H.; Zhou, Y. Impact of Climate Change on the Division of Flood Season. *Water Power* **2018**, *44*, 22–26.
40. He, H.; Zhang, A. The application of Fisher method to dividing seismicity period in yunnan province. *J. Seismol. Res.* **1994**, *17*, 231–239.
41. Wu, J.; Sheng, Z.; Du, J.; Zhang, Y.; Zhang, J. Spatiotemporal Change Patterns of Temperature and Precipitation in Northeast China from 1956 to 2017. *Res. Soil Water Conserv.* **2021**, *28*, 340–347+415. [\[CrossRef\]](#)

Disclaimer/Publisher's Note: The statements, opinions and data contained in all publications are solely those of the individual author(s) and contributor(s) and not of MDPI and/or the editor(s). MDPI and/or the editor(s) disclaim responsibility for any injury to people or property resulting from any ideas, methods, instructions or products referred to in the content.